

Quantitative analysis of projectile deformation using 3D close range photogrammetry: geometric modeling, statistical caliber inference, and forensic target classification

S.T. Costa ^a, C.T. Arrabal^a, R.H. O. Montes^a and R.R. Cunha ^{a*}

^a Instituto de Criminalística, Superintendência de Polícia Técnico Científica de São Paulo, Brasil

*Endereço de e-mail para correspondência: rafaelperitocriminal@gmail.com. Tel.: +55-34-991581119

Recebido em 06/04/2026; Revisado em 10/06/2026; Aceito em 12/06/2026

Resumo

Este estudo avaliou a aplicação da fotogrametria tridimensional como método quantitativo para análise de deformação de projéteis de arma de fogo após impacto em diferentes materiais. Foram empregados projéteis encamisados dos calibres 9 mm Luger, .380 Auto, .38 SPL e .40 S&W, disparados contra alvos distintos em múltiplas distâncias. A partir dos modelos tridimensionais reconstruídos, adotou-se como variável principal o volume relativo fotogramétrico, do qual se derivou a deformação específica geométrica (ϵ_g), grandeza adimensional capaz de expressar compressão aparente, expansão aparente ou conservação morfológica relativa do projétil remanescente. Os dados foram submetidos à análise de variância com o modelo $\epsilon_g \sim \text{Calibre} + \text{Material} + \text{Distância}$. Os resultados indicaram efeito estatisticamente significativo de calibre e material sobre a deformação, enquanto a distância não apresentou efeito significativo. A análise Post Hoc evidenciou grupos homogêneos entre calibres e materiais, permitindo inferências sobre distinguibilidade. Observou-se padrão deformacional distinto entre os alvos, permitindo a proposição de uma tipologia forense baseada em conservação morfológica, deformação plástica expansiva e fragmentação catastrófica.

Palavras-Chave: Fotogrametria de curto alcance; Tridimensionalização; Distância de disparo; Deformação Balística.

Abstract

This study investigates the use of three-dimensional photogrammetry as a quantitative method for assessing projectile deformation after impact against different target materials. Full metal jacket projectiles of four calibers (9 mm Luger, .380 Auto, .38 SPL and .40 S&W) were fired against distinct substrates at distances ranging from 5 m to 40 m. From the reconstructed three-dimensional models, a relative volumetric parameter was defined and used to derive a dimensionless geometric deformation index (ϵ_g), capable of representing apparent compression, apparent expansion or relative morphological preservation of the projectile. The dataset was analyzed using a multifactorial analysis of variance model ($\epsilon_g \sim \text{caliber} + \text{material} + \text{distance}$). The results indicate statistically significant effects of caliber and material on deformation, whereas shooting distance did not present a significant effect within the tested range. Post hoc comparisons revealed homogeneous groups among calibers and materials, highlighting limitations in distinguishing certain calibers based solely on deformation. A consistent deformation pattern associated with target type was observed, allowing the proposal of a forensic typology of materials based on mechanical response regimes. The integration of photogrammetry, geometric modeling and statistical inference provides a robust framework for quantitative interpretation of projectile deformation in forensic contexts.

Keywords: Close Range Photogrammetry; Tridimensionalization; firing distance; Ballistic deformation.

1. INTRODUCTION

According to data from 2016, the use of firearms has been one of the greatest contributions to the number of deaths in the world [1]. In 2019, 70% of homicides registered in Brazil were caused by firearms [2]. In

addition to these circumstances, another survey from 2020 shows that 70% of murder cases are not punished in Brazil [3] and the most predilect region for it is the back of the head (occipital bone) [4].

Most recently, trace elements resulting from gunshots residues (GSR) can be analyzed through distinct methods,

overcoming the ancient colorimetric methods that should be in decay in Brazil [5] with such as gunshot residues (GSR) on clothes and suspect hands/body [6]. Aiming towards projectile, finite element analysis [7] and imaging data [8-9] has proven to be promising tools. Through qualitative and quantitative studies, were evaluated the shooting distance estimation based on gunshot residues analyzed by X-Ray diffraction and multivariate analysis [10] and determination of firing distance and firing angle by neutron activation analysis [11].

In this scenario, it is essential to strengthen police strategies for identification and capture of suspects who have practiced crimes involving firearms. It is also of fundamental importance the development of accessible technologies [12] that can assess the traces present in a crime scene involving a firearm and that can assist in the elucidation of criminal occurrences that are easily accessible to police enforcement, mainly crime scene experts.

Using photogrammetry with forensic applications is not new [13]. Thus, an alternative as an ally in expert analysis is the application of the close-range photogrammetry technique that consists of extracting 3D information from physical objects, such as a firearm projectile, through photographic images. It is an easily accessible technique, since it can be performed using digital cameras and even using smartphone device cameras [14].

In this context, three-dimensional photogrammetry emerges as a promising complementary technique, enabling non-destructive, reproducible and high-resolution geometric reconstruction of deformed projectiles to estimate the firing distance. Unlike traditional approaches based on visual inspection or limited linear measurements, 3D photogrammetry allows a volumetric interpretation of deformation, offering new possibilities for quantitative analysis.

2. OBJECTIVE

The objective of this study was to develop a simple, fast and low-cost photogrammetry-based procedure to assess projectile deformation against different targets, calibers and shooting distances, and to establish relationships based on relative deformation changes.

3. MATERIALS AND METHODS

The interpretation of projectile deformation requires careful conceptual consideration. As a general rule, the mass of a recovered projectile tends to remain constant, except in cases involving material loss due to abrasion or fragmentation. The behavior of volume, however, must be treated with greater rigor. In metals subjected to plastic

deformation, it is more appropriate to consider an approximate conservation of material volume accompanied by significant geometric redistribution, rather than an intrinsic reduction in volume.

For this reason, photogrammetry should not be simplistically presented as a tool to demonstrate mere “volume reduction” of a projectile. The method does not measure absolute volume (mm^3), but rather a relative or normalized volume. What it captures more reliably is the external geometric transformation of the body after impact, including flattening, lateral expansion, surface irregularities, and loss of symmetry. Any volumetric difference observed in three-dimensional models should therefore be interpreted as apparent geometric variations, influenced by final shape, internal voids, localized material loss, or reconstruction limitations, rather than as direct physical compression of the metal.

Within this framework, it is proposed to adopt the parameter geometric compressive strain, a dimensionless quantity, as a more appropriate descriptor of the relative variation between the original and deformed configurations of the projectile. This approach is more consistent with the principles of solid mechanics and more defensible in both forensic and scientific contexts.

3.1. Mathematical Modeling

The variable “Volume” should be interpreted as a three-dimensional relative volume, that is, a ratio between the three-dimensional reconstructed volume of the projectile after impact and a reference volume of the undeformed projectile obtained through 3D photogrammetry, as shown in Figure 1. Under this perspective, the parameter no longer represents an absolute volume, but rather expresses a comparative measure of the geometric alteration of the body after collision. This interpretation is particularly useful because it transforms deformation into a dimensionless quantity, enabling comparisons across different calibers and impact surfaces without direct dependence on the absolute size of the projectile.

Considering a projectile with known or estimable original geometry, the geometric compressive strain is defined as:

$$\varepsilon_g = (V_0 - V_d) / V_0 \quad \text{Equation 1}$$

where (ε_g) is the geometric compressive strain, (V_0) is the reference geometric volume of the intact projectile, and (V_d) is the geometric volume of the deformed projectile reconstructed through photogrammetry. This is a dimensionless quantity that expresses the relative variation between the initial and final configurations.

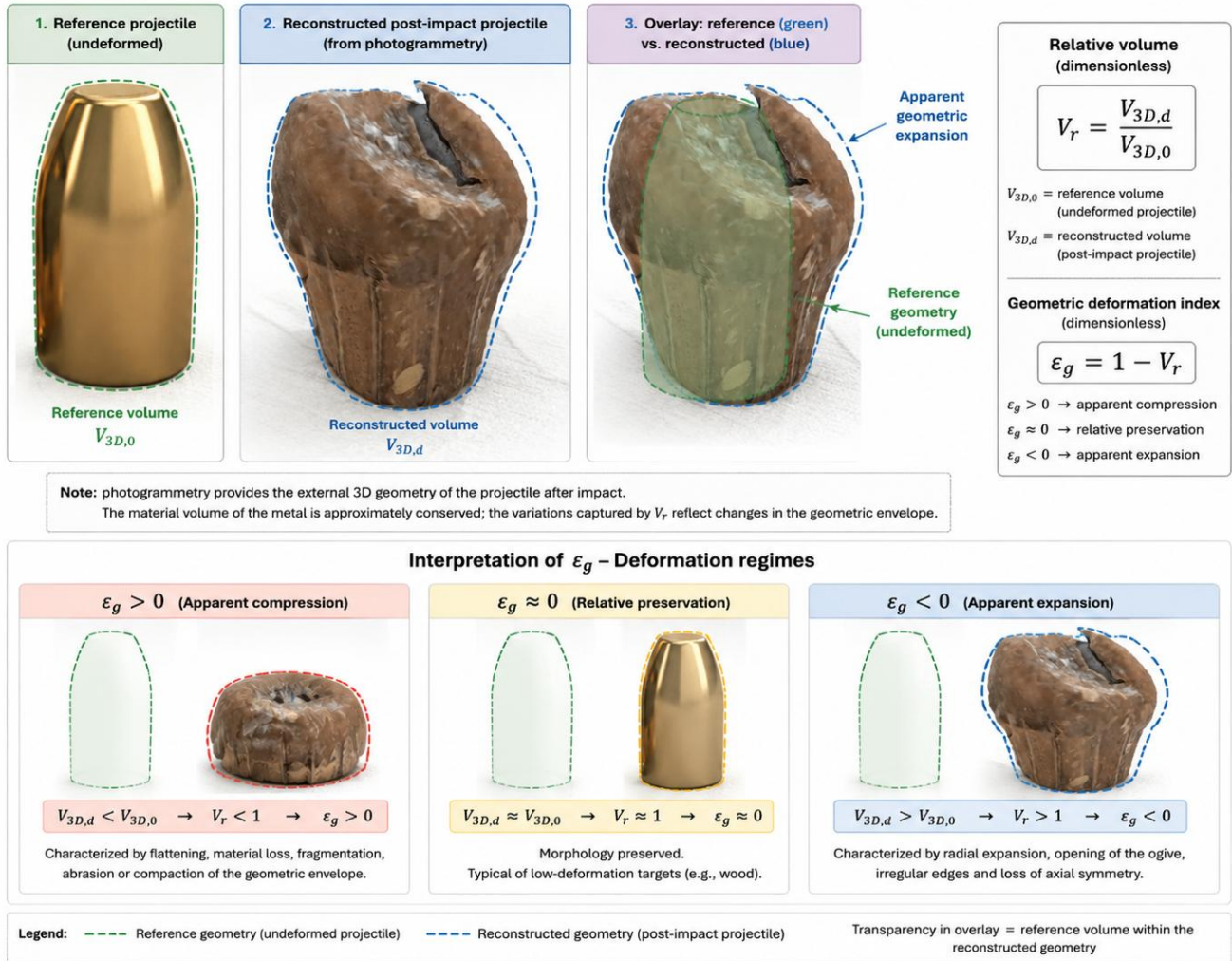


Figure 1. Infogram of the relative volume concept used in this study. Generated by IA.

3.1. Field experiment

A total of 480 experimental shots were performed using full metal jacket ammunition in four calibers: 9 mm Luger, .380 Auto, .38 SPL and .40 S&W. The projectiles were kindly donated by Companhia Brasileira de Cartuchos (CBC), the extension in projectiles deformation reproducibility were ensured by firing at least three times (reproducibility) against four distinct materials as targets (plywood, steel plate, clay brick wall and concrete brick wall) at four ranges (5 m, 10 m, 20 m, 30 m and 40 m).

After hitting the target, each projectile was searched for, if found, collected, tagged and individualized in small plastic bags, according to target surface and distance.

Approximately 25% of the projectiles were successfully recovered, the remaining were either disintegrated through fragmentation by the impact or lost inside / around the targets. Impacts against steel plates resulted in extensive fragmentation, preventing further geometric analysis, whereas projectiles recovered from

wood showed minimal deformation and preserved their original morphology, including rifling marks.

The recovered projectiles were subjected to a photogrammetric acquisition protocol involving controlled multi-view imaging and subsequent reconstruction using specialized software. From the reconstructed models, a relative volume parameter was defined as the ratio between the volume of the deformed projectile and a reference volume corresponding to its undeformed state (Figure 1 and Table 1). Based on this parameter, a geometric deformation index was defined as $\epsilon_g = 1 - V_r$, where V_r represents the relative volume as the ratio $V_r = V_{d \text{ deformed reconstructed}} / V_{0 \text{ original reference}}$. This dimensionless variable allows classification of deformation into apparent compression ($\epsilon_g > 0$), relative preservation ($\epsilon_g \approx 0$) and apparent expansion ($\epsilon_g < 0$).

In the present study, the term reconstructed volume refers to the geometric volume calculated from the three-dimensional mesh generated through photogrammetric reconstruction of the recovered projectile after impact. Therefore, the method does not directly measure the physical volume of the metallic material itself, but rather the external geometric envelope represented by the

reconstructed digital model. A schematic representation of the relationship between the undeformed reference projectile and the reconstructed post-impact geometry is provided in [Figure 1](#).

Due to the partial recovery of projectiles, the dataset presented an intrinsically unbalanced structure. Therefore, a multifactorial analysis of variance was applied using the model ε_g as a function of caliber, material and distance, with caliber also treated as a blocking factor to account for its intrinsic heterogeneity.

3.2. Photogrammetric Processing

A trial for 90 days of 3D Zephyr 5.019 version were kindly donated from 3D Flow (Verona, Italy). Eight (8) Control Points (CP) were printed in a round distribution from the template available in 3D Zephyr photogrammetry software within a 3.2 cm central grid to be a fixed scale where the projectile was placed to perform photographs. The images were then processed using 3DF Zephyr software, employing a three-dimensional reconstruction workflow based on dense point clouds and polygonal mesh generation. All projectiles were registered upon the fixed scale in a rotary plate ([Figure 2](#)). Thus, about 35 pictures were taken from 360° view. The pictures underwent to 3DF Zephyr software in order to rebuild the digital twin of the damaged bullet ([Table 1](#)). The presets were always the higher as they were available by the software.

From the reconstructed 3D models, deformation measurements were extracted by assessing geometric deviations relative to the original projectile shape.

3.3. Data Acquisition and setup

After firing, the projectiles were collected and subjected to photographic image acquisition from multiple angles. Calibration cubes were used to ensure proper scale and dimensional accuracy. In total, the dataset comprised was 4,262 image files resulting in 13.3 GB of data. For capturing the images, a cellphone Samsung Galaxy Note 20 Ultra camera was employed, and processed in a notebook AVEL (Brasil) with 16 GB of RAM, CPU Intel I7 10750H @2.60 GHz, and GPU Nvidia GForce GTX 2060i with 6 GB RAM.



Figure 2. Rotary plate with a projectile being photographed with the round fixed scale.

3.4. Statistical Analysis

All measurements were inserted in an MS Excel sheet.

The data were analyzed using descriptive statistics with multiple comparison tests (bootstrap) and Analysis of variance (ANOVA). A significance level of 5% ($p < 0.05$) was adopted for all statistical tests.

Table 1. Three dimensional 9mm Luger projectiles with relative deformation after being shot against clay brick in distances of 5, 10, 20, 30 and 40 meters, at least three times.



4. RESULTS AND DISCUSSION

In order to test the robustness of the proposed method, the same deformed .38 SPL fired from 30m against clay brick were analyzed by the same photographer and same 3D analyst. The inter-day repeatability results demonstrate a high level of robustness and reliability of the proposed photogrammetric method. For the same projectile condition (30 m, A, .38 SPL), analyzed by the same operator and using the same acquisition protocol, the measured values of volume across three different days (1.333412, 1.332471, and 1.343326) show minimal variation. The resulting mean value of 1.336403, combined with an extremely low relative standard deviation ($RSD \approx 0.006\%$), indicates excellent measurement consistency and negligible inter-day variability. This level of precision suggests that the method is not significantly influenced by temporal factors such as lighting conditions, operator handling, or minor environmental variations. Consequently, the photogrammetric workflow can be considered highly stable and reproducible, supporting its application as a reliable quantitative tool in forensic analysis of projectile deformation.

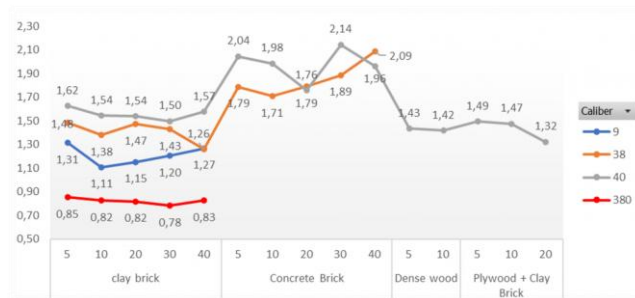


Figure 3. Mean deformation in each material and distances.

The descriptive analysis presented in Figure 3 provides important insight into the behavior of the geometric deformation index before formal statistical testing. When all calibers and target materials are considered simultaneously, a clear separation among calibers can be observed. The .40 S&W consistently produced the highest relative volume values, with an overall mean of 1.66, followed by the .38 SPL (1.60), the 9 mm Luger (1.21), and the .380 AUTO (0.82). This pattern indicates the existence of an intrinsic heterogeneity associated with projectile caliber, suggesting that projectile construction, mass, and impact energy influence the final geometric response after impact.

A similar behavior is observed for target materials. Concrete brick produced the highest overall deformation values (mean = 1.90), whereas clay brick (1.26), plywood + clay brick (1.40), and dense wood (1.43) showed

substantially lower and relatively similar responses. These findings suggest that the mechanical properties of the target exert a stronger influence on projectile deformation than the shooting distance itself. In practical terms, impacts against concrete tended to produce greater apparent geometric expansion of the reconstructed projectile envelope, while wood and plywood were associated with greater preservation of the original morphology.

Conversely, the analysis of deformation as a function of distance reveals a remarkably stable pattern. The mean relative volume varied only from 1.41 to 1.49 across the investigated range of 5 m to 40 m, corresponding to less than 6% variation. This limited fluctuation contrasts sharply with the differences observed between calibers and materials, which frequently exceeded 30–50%. Such behavior provides an initial indication that shooting distance contributes relatively little to the observed deformation pattern within the experimental interval considered.

Figure 2 further illustrates this phenomenon. Although local increases and decreases can be observed for specific combinations of caliber and material, particularly for .38 SPL and .40 S&W impacting concrete brick, no systematic monotonic trend is evident as distance increases. Instead, deformation values oscillate around material-dependent levels, suggesting that target composition governs the dominant deformation mechanism. These observations are consistent with the subsequent ANOVA results, which identified significant effects for caliber and material but not for shooting distance.

The practical forensic implication is that projectile morphology appears to preserve information about the nature of the impacted target and, to a lesser extent, about projectile caliber, whereas shooting distance within the range of 5–40 m does not generate a sufficiently distinct geometric signature to allow reliable discrimination. Consequently, deformation patterns should be interpreted primarily as indicators of projectile–target interaction rather than as direct estimators of firing distance.

Some projectiles were not recovered after the shooting while others were found to undergo fragmentation, leaving pieces of the inner core or even only the jacket. When shooting with a .40 S&W against concrete brick, 20% of the shoots were either fragmentation or jacket only. While shooting with .38 SPL has shown only 13% of fragmentation against concrete brick. No fragmentation or jacket only were observed when shoots were fired against clay brick (Table 2).

The raw data presented in Table 2 were compiled with the mean and RSD in Table 3. Its results show that some percentual RSD were above 10%, meaning that there was a high presence of heterogeneous results, even with the

same shooter and gun, same surface and same ammunition. Still, the results have shown distinct values for some and provide the data to build the **Figure 4**.

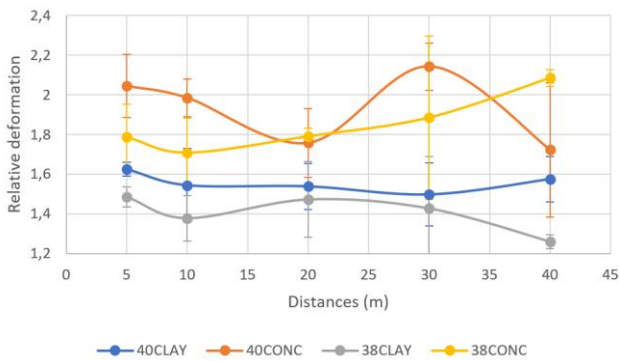


Figure 4. Graphical results from the comparison between .38 SPL and .40 S&W fired against concrete or clay bricks.

The graphical analysis of volumes reconstructed through photogrammetry further demonstrates that the target material exerts a predominant influence on projectile deformation behavior, while shooting distance, within the analyzed range, does not present a systematic trend. Impacts on concrete results in significantly higher relative volume values, indicating a predominance of apparent geometric expansion, whereas impacts on clay brick yield values closer to unity, consistent with moderate deformation and greater morphological stability. Additionally, the larger error bars observed in concrete tests indicate a more heterogeneous behavior, likely associated with the fracturable nature of the material and local variability in projectile–target interaction. These findings reinforce the interpretation that geometric deformation, as expressed by the proposed parameter, is strongly dependent on the type of target substrate and only weakly influenced by shooting distance under the experimental conditions considered.

The analysis of the relative standard deviation (RSD) values indicates that projectile geometric deformation depends not only on the mean relative volume but also on the stability of the deformation process under each experimental condition. It is observed that tests conducted on clay brick tend to exhibit lower RSD values, particularly for the .40 S&W caliber at shorter distances (approximately 2–12%), indicating a more predictable and consistent behavior. In contrast, tests performed on concrete show significantly higher RSD values, reaching approximately 19.6% for .40 S&W at 40 m and 21.8% for .38 SPL at 30 m, which reflects a high dispersion of results. This increase in variability suggests that concrete induces a deformation regime that is highly sensitive to local micro-variations at impact, such as structural heterogeneity of the material, angle of incidence, and fracture points. Therefore, in addition to promoting higher mean deformation, concrete is also characterized by lower

predictability, reinforcing its classification as a substrate associated with heterogeneous plastic deformation.

Furthermore, although shooting distance did not show a statistically significant effect in the overall ANOVA, local patterns of deformation instability are observed for specific combinations of caliber and material. For instance, in concrete, the .40 S&W caliber exhibits a marked increase in variability at longer distances, while the .38 SPL shows intermediate peaks of dispersion at distances between 20 m and 30 m. This behavior suggests that, under certain conditions, distance may act as a modulating factor in the stability of deformation, even if it does not significantly affect the mean relative volume. From a physical standpoint, this may be related to the reduction in impact velocity and the consequent transition from a more uniform deformation regime to one dominated by localized fractures and asymmetric deformation patterns. Thus, although distance does not directly determine the magnitude of deformation, it may influence the consistency of the deformation pattern, which is relevant for forensic interpretation in real-world scenarios.

Continuing with the statistic treatment, the analysis of variance revealed a strong effect of both material and caliber on the geometric deformation index. The material factor presented an F value of 104.24 ($p < 0.001$), while caliber showed an F value of 69.12 ($p < 0.001$), indicating that both variables significantly influence projectile deformation. In contrast, shooting distance did not show a statistically significant effect within the studied range.

The analysis of variance revealed a strong effect of both material and caliber on the geometric deformation index. The material factor presented an F value of 104.24 ($p < 0.001$), while caliber showed an F value of 69.12 ($p < 0.001$). The F statistic represents the ratio between the variance explained by a given factor and the residual variance observed within groups. Therefore, an F value of approximately 104 indicates that the variability associated with target material is more than one hundred times greater than the variability observed within individual experimental groups, highlighting the dominant influence of material on projectile deformation. In contrast, shooting distance did not show a statistically significant effect within the studied range.

Model assumptions were evaluated through Shapiro-Wilk and Breusch-Pagan tests. The Shapiro-Wilk test indicated no significant departure from normality ($p = 0.0789$), suggesting that the residuals were approximately normally distributed. Likewise, the Breusch-Pagan test indicated homogeneity of variances ($p = 0.9776$), supporting the assumption of homoscedasticity. Together, these results validate the application of ANOVA and increase confidence in the reliability of the statistical

inferences. The model explained approximately 85% of the observed variability.

Post hoc comparisons using bootstrap methods revealed that .40 S&W and .38 SPL belong to the same statistical group, showing no significant difference between their mean deformation values. In contrast, 9 mm Luger and .380 Auto formed distinct groups, with significantly lower deformation. Regarding materials, concrete brick formed a distinct group with the highest deformation, while clay brick, dense wood and plywood combinations showed no significant differences among themselves.

Revisiting at Equation 01, from this perspective, two distinct deformation regimes can be identified. When $\epsilon_g > 0$, a compressive regime is observed, corresponding to apparent volumetric reduction dominated by axial flattening. When $\epsilon_g < 0$, an expansive regime is identified, characterized by an increase in reconstructed volume associated with irregular deformation or partial fragmentation. A conservative regime may also be defined when $\epsilon_g \sim 0$, indicating minimal deformation and preservation of the original geometry.

These regimes allow a classification of deformation behavior: compressive ($\epsilon_g > 0$) associated with dominant flattening; conservative ($\epsilon_g \sim 0$) associated with negligible deformation, as observed in plywood; and expansive ($\epsilon_g < 0$) associated with irregularity or partial fragmentation.

The overall analytical framework is therefore based on evaluating the relationship:

$$\epsilon_g \sim \text{Caliber} + \text{Material} + \text{Distance} \quad \text{Equation 2}$$

That includes interaction effects between material and caliber, and the derivation of deformation behavior curves for each material.

For example, wood tends to produce $\epsilon_g \sim 0$, indicating morphological preservation, whereas concrete tends to produce positive values associated with compressive deformation, and steel results in non-measurable conditions due to fragmentation.

This framework naturally leads to a forensic typology of target materials and enables practical interpretative questions, such as which caliber exhibits greater deformation in concrete, and which calibers maintain structural integrity when impacting wood.

The data further suggest that the interpretation of ϵ_g should always be considered in conjunction with the nature of the target. When the impacted surface favors morphological preservation, as in wood, values near neutrality carry greater physical meaning. When the target promotes crushing, surface cracking, abrasion, or peripheral spreading, as observed in ceramic and cementitious substrates, the sign and magnitude of ϵ_g become even more informative, distinguishing between apparent compaction of the remaining structure and geometric expansion of the deformed envelope. This reinforces the hypothesis that photogrammetry, combined with dimensionless geometric indices, can function as an objective tool for comparing impact patterns in terminal ballistics.

Finally, the use of this modeling approach contributes to aligning forensic analysis with the language of solid mechanics without compromising practical applicability. Rather than stating that a projectile “lost volume” or “increased in size by deformation,” this method can more rigorously assert that a variation in reconstructed relative volume occurred, expressed as positive, negative, or near-zero geometric specific deformation (ϵ_g), depending on the dominant morphological regime.

Table 2. Three dimensional results of relative deformation of ~15 full metal jacket of .40 S&W and .38 SPL caliber (n=3 or 4) shots against clay and concrete brick (5m to 40m). “Jacket only” stands for no inner core found, and “Frag” stands for total fragmentation.

		Clay Brick .40 S&W	Concrete Brick .40 S&W	Clay Brick .38 SPL	Concrete Brick .38 SPL
5 m	5A	1.628977	2.013227	1.540523	1.612766
	5B	1.587137	2.216554	1.443092	1.80195
	5C	1.65684	1.904339	1.470928	1.944396
10 m	10A	1.657094	Jacket only	1.296339	1.581174
	10B	1.601537	Frag	1.508841	1.907201
	10C	1.278482	1.917153	1.327606	1.636198
	10D	1.542699	2.051782		
20 m	20A	1.521133	1.882860	1.744212	1.760359
	20B	1.59353	1.535153	1.301242	1.820859

20 m	20C	1.634838	1.707461	1.424823	Frag
	20D	1.394073	1.905571		
30 m	30A	1.673008	2.192041	1.333412	1.544858
	30B	1.452487	2.230492	1.722717	2.342953
	30C	1.36625	2.006304	1.223845	1.767803
40 m	40A	1.706496	1.962789	1.298137	2.055444
	40B	1.491386	Frag	1.238509	2.114980
	40C	1.526547	1.483907	1.239927	Frag

Graphical analysis further demonstrated that deformation values are consistently higher in concrete than in clay brick. For instance, when averaging the measurements obtained across all analyzed shooting distances, the mean relative volume increased from approximately 1.41 to 1.84 for .38 SPL and from 1.55 to 1.96 for .40 S&W when transitioning from clay brick to concrete brick. These values are summarized in [Figure 2](#) and [Tables 2-3](#). The variability, as measured by relative standard deviation, was also higher in concrete, indicating a more heterogeneous deformation process.

The results indicate that projectile deformation should be interpreted primarily as a geometric transformation rather than a change in intrinsic material volume. The proposed deformation index ε_g reflects changes in the reconstructed geometric envelope of the projectile, which arise from plastic deformation, lateral expansion, surface irregularities and loss of symmetry, rather than true volumetric compression of the metallic material.

The graphical analysis confirms that target material is the dominant factor governing deformation behavior. Concrete induces higher relative volumes and therefore more negative ε_g values, corresponding to apparent geometric expansion. Clay brick produces intermediate deformation with greater stability, while wood tends to preserve the original morphology of the projectile. Steel, in turn, represents a distinct regime characterized by catastrophic fragmentation, in which geometric modeling becomes impractical.

The analysis of variability reinforces this interpretation, as concrete exhibits higher dispersion, reflecting sensitivity to local heterogeneities and fracture patterns. Clay brick, on the other hand, produces more consistent deformation, suggesting a more predictable interaction between projectile and target.

The dataset also reveals intrinsic heterogeneity associated with caliber. The .380 Auto exhibits deformation values approximately half those of the .40 S&W, indicating fundamentally different deformation scales. This heterogeneity justifies the strong statistical effect of caliber and supports its use as a blocking factor in the model.

At the same time, the similarity of deformation values across distances confirms that, within the tested range, distance does not significantly influence the deformation regime. Although minor fluctuations are observed, they do not form a systematic trend and are insufficient to produce statistical significance.

From a forensic perspective, these findings suggest that deformation is more informative for identifying target material when it is concrete than for distinguishing between certain calibers ([Table 4](#)). The inability to statistically differentiate between .40 S&W and .38 SPL based solely on deformation highlights the need for complementary analyses. Conversely, the distinct behavior of concrete supports its identification as a high-deformation substrate.

However, using Bootstrap Multiple Comparison test for caliber allow to distinguish between .38 SPL, .380 AUTO and 9mm Luger since their 3D deformation means can be separated into 3 distinct groups ([Table 5](#)). These findings can be helpful when there is no information of the caliber beyond just the mass, the base diameter, and now with the deformation and material target we could diagnose more precisely caliber.

Based on these results, a forensic typology of targets can be proposed. Wood corresponds to a regime of morphological preservation, clay brick to moderate and stable deformation, concrete to intense and heterogeneous plastic deformation, and steel to fragmentation-dominated behavior.

Table 3. Three-dimensional results of relative deformation mean distribution for distances from 5m to 40m (n=3 or 4) with error.

.40 Clay Brick				.40 Concrete Brick			
Distance	Mean	RSD	%	Distance	Mean	RSD	%
5	1.624318	0.035084281	2.159939178	5	2.044706667	0.158470119	7.750261765
10	1.5437392	0.186829632	12.10240903	10	1.9844675	0.095197079	4.797109494
20	1.537892833	0.115004995	7.478089009	20	1.75776125	0.172802361	9.830820919
30	1.497248333	0.158201771	10.56616778	30	2.142945667	0.119886733	5.594483073
40	1.574809667	0.115390822	7.327286866	40	1.723348	0.33862071	19.64900354

.38 Clay Brick				.38 Concrete Brick			
Distance	Mean	RSD	%	Distance	Mean	RSD	%
5	1.484847667	0.050184836	3.379796951	5	1.786370667	0.16636301	9.312905359
10	1.377595333	0.114732189	8.328439111	10	1.708191	0.174529783	10.21722882
20	1.47207575	0.190084636	12.91269393	20	1.790609	0.04277996	2.389129076
30	1.426658	0.262182056	18.37735855	30	1.885204667	0.411796395	21.84359089
40	1.258857667	0.034024288	2.702790737	40	2.085212	0.042098309	2.018898286

Finally, the recovery rate of approximately 25% is not merely a limitation but an inherent aspect of the physical process. The feasibility of quantitative analysis depends on the impact regime, emphasizing the need to consider recovery probability as part of the experimental and forensic framework.

Table 4. Bootstrap Multiple Comparison test for material.

Group	Material	Mean
A	Concrete Brick	1.902
B	Dense wood	1.427
B	Plywood + Clay Brick	1.400
B	Clay brick	1.264

Table 5. Bootstrap Multiple Comparison test for caliber.

Group	Caliber	Mean
A	.40 S&W	1.656
A	.38 SPL	1.600
B	9mm LUGER	1.211
C	.380 AUTO	0.822

The descriptive analysis presented in **Figure 3** and **Tables 6–7** provides important insight into the behavior of the geometric deformation index before formal statistical testing. When all calibers and target materials are considered simultaneously, a clear separation among calibers can be observed. The .40 S&W consistently

produced the highest relative volume values, with an overall mean of 1.66, followed by the .38 SPL (1.60), the 9 mm Luger (1.21), and the .380 AUTO (0.82). This pattern indicates the existence of an intrinsic heterogeneity associated with projectile caliber, suggesting that projectile construction, mass, and impact energy influence the final geometric response after impact.

A similar behavior is observed for target materials. Concrete brick produced the highest overall deformation values (mean = 1.90), whereas clay brick (1.26), plywood + clay brick (1.40), and dense wood (1.43) showed substantially lower and relatively similar responses. These findings suggest that the mechanical properties of the target exert a stronger influence on projectile deformation than the shooting distance itself. In practical terms, impacts against concrete tended to produce greater apparent geometric expansion of the reconstructed projectile envelope, while wood and plywood were associated with greater preservation of the original morphology.

Conversely, the analysis of deformation as a function of distance reveals a remarkably stable pattern. The mean relative volume varied only from 1.41 to 1.49 across the investigated range of 5 m to 40 m, corresponding to less than 6% variation. This limited fluctuation contrasts sharply with the differences observed between calibers and materials, which frequently exceeded 30–50%. Such behavior provides an initial indication that shooting distance contributes relatively little to the observed

deformation pattern within the experimental interval considered.

Although local increases and decreases can be observed (Figure 3) for specific combinations of caliber and material, particularly for .38 SPL and .40 S&W impacting concrete brick, no systematic monotonic trend is evident as distance increases. Instead, deformation values oscillate around material-dependent levels, suggesting that target composition governs the dominant deformation mechanism. These observations are consistent with the ANOVA results, which identified

significant effects for caliber and material but not for shooting distance.

The practical forensic implication is that projectile morphology appears to preserve information about the nature of the impacted target and, to a lesser extent, about projectile caliber, whereas shooting distance within the range of 5–40 m does not generate a sufficiently distinct geometric signature to allow reliable discrimination. Consequently, deformation patterns should be interpreted primarily as indicators of projectile–target interaction rather than as direct estimators of firing distance.

Table 6. Relative deformation: natural heterogeneity among CALIBER vs TARGET.

	Caliber			
Material	9 mm	.380	.38	.40
Clay Brick	1.21	0.82	1.41	1.55
Concrete Brick	-	-	1.84	1.96
Dense Wood	-	-	-	1.43
Plywood + Clay Brick	-	-	-	1.40
Total	1.21	0.82	1.60	1.66

Table 7. Relative deformation: similarity for DISTANCE vs TARGET.

	Distance				
Material	5 m	10 m	20 m	30 m	40 m
Clay Brick	1.28	1.26	1.30	1.23	1.24
Concrete Brick	1.92	1.82	1.77	2.01	2.02
Dense Wood	1.43	1.42	-	-	-
Plywood + Clay Brick	1.49	1.47	1.32	-	-
Total	1.48	1.41	1.41	1.49	1.41

Even more, although the proposed geometric deformation index provides an objective and quantitative description of projectile morphology after impact, its forensic interpretation should not be performed in isolation. Projectile deformation is influenced by multiple factors, including target composition, impact angle, projectile construction, intermediate targets, ricochets, and fragmentation processes. Consequently, similar deformation patterns may arise from distinct ballistic scenarios. For this reason, conclusions regarding shooting reconstruction should always be supported by an integrated analysis of all available evidence, including projectile trajectories, impact sites, cartridge case distribution, firearm characteristics, scene documentation, and associated trace evidence. The proposed methodology should therefore be considered as a complementary forensic tool capable of strengthening, but not replacing, comprehensive ballistic reconstruction.

5. CONCLUSION

The proposed framework bridges experimental ballistics and quantitative geometric analysis, offering a reproducible and scalable approach for forensic applications.

The integration of three-dimensional close-range photogrammetry, geometric modeling and statistical analysis provides a robust framework for the quantitative assessment of projectile deformation.

The results demonstrate that deformation is primarily governed by caliber and target material, while shooting distance plays a limited role within the tested range. Photogrammetry has shown the expected result concerning lower mass and energy with smaller deformations. The .380 AUTO deforms less than 9mm Luger, showing potential to differentiate both calibers with similar projectile diameter, while .40 S&W and .38 SPL present similar deformation. On the other hand,

distinct distances from 5m to 40m did not affect the relative compression of the slugs (P -valor > 0.05).

A limitation of the present study is the partial recovery rate (~25%), which may introduce selection bias toward measurable deformation regimes

The proposed geometric deformation index offers a consistent and interpretable parameter for comparative analysis, supporting both scientific investigation and forensic application. The methodology enables the classification of target materials based on deformation patterns and highlights the potential of photogrammetry as an advanced tool in forensic ballistics.

ACKNOWLEDGMENTS

The authors would like to thank CBC for the donation of all ammunition and the CTC at Ribeirão Pires SP for lending the shooting range. Also, to the 3DFlow for granting the trial of the 3DF Zephyr software.

REFERENCES

- [1] Global Burden of Disease 2016 Injury Collaborators. Global mortality from firearms, 1990–2016. *J. Am. Med. Assoc.* 764: 792–814 (2018). <https://doi.org/10.1001/jama.2018.10060>.
- [2] Brasil, Ministério da Saúde. Banco de dados do Sistema Único de Saúde – DATASUS. Available at: <http://www.datasus.gov.br> (accessed March 25, 2021).
- [3] Instituto Sou da Paz. Onde mora a impunidade. Available at: <http://soudapaz.org/o-que-fazemos/conhecer/pesquisas/politicas-de-seguranca-publica/control-de-homicidios/?show=documentos#3969> (accessed March 25, 2021).
- [4] T.L. Espicalsky; S.T. Costa; M. Crivelli. Craniofacial injuries by firearm projectiles: analysis of cases in Brazil. *J. Forensic Leg. Med.* 69: (2020)
- [5] ASSOCIAÇÃO BRASILEIRA DE CRIMINALÍSTICA (ABC). Parecer técnico: revogação da técnica colorimétrica rodizonato de sódio para análise de resíduos de disparo de arma de fogo (Recomendação Técnica – GSR). Brasília: ABC, 2021
- [6] S.V.F. Castro; A.P. Lima; R.G. Rocha; R.M. Cardoso; R.H.O. Montes; M.H.P. Santana; E.M. Richter; R.A.A. Munoz. Simultaneous determination of lead and antimony in gunshot residue using a 3D-printed platform working as sampler and sensor. *Anal. Chim. Acta* 1130: 126-136 (2020). <https://doi.org/10.1016/j.aca.2020.07.033>
- [7] S.T. Costa; A.R. Freire; B.C. Ferreira-Pileggi; E. Daruge Júnior; F.B. Prado; A.C. Rossi. Finite element analysis dynamic simulation of projectile impact caliber .40 S&W in temporal bone with neural tissue. *Aust. J. Forensic Sci.* 56: 189-200 (2024).
- [8] J. Kumar; D. Landheer; J. Barnes-Warden; P. Fenne; A. Attridge; M.A. Williams. Inconsistency in 9 mm bullets measured with non-destructive X-ray computed tomography. *Forensic Sci. Int.* 214: 48-58 (2012).
- [9] J. Thornby; D. Landheer; T. Williams; J. Barnes-Warden; P. Fenne; D. Norman; A. Attridge; M.A. Williams. Inconsistency in 9 mm bullets: correlation of jacket thickness to post-impact geometry measured with non-destructive X-ray computed tomography. *Forensic Sci. Int.* 234: 111-119 (2014).
- [10] K.L. Miranda; F.E. Ortega-Ojeda; C. García-Ruiz; P.S. Martínez. Shooting distance estimation based on gunshot residues analyzed by XRD and multivariate analysis. *Chemometr. Intell. Lab. Syst.* 193: 103831 (2019).
- [11] G. Capannesi; C. Ciavola; A.F. Sedda. Determination of firing distance and firing angle by neutron activation analysis in a case involving gunshot wounds. *Forensic Sci. Int.* 61: 75–84 (1993). [https://doi.org/10.1016/0379-0738\(93\)90216-w](https://doi.org/10.1016/0379-0738(93)90216-w).
- [12] R.R. Cunha; C.T. Arrabal; M.M. Dantas; H.R. Bassaneli. Laser scanner and drone photogrammetry: a statistical comparison between 3-dimensional models and its impacts on outdoor crime scene registration. *Forensic Sci. Int.* 330: 111100 (2021).
- [13] M. Urbanová; P. Hejna; J. Zátoková; M. Kozák. Application of photogrammetry in forensic science. *Forensic Sci. Int.* 264: 77–84 (2016).
- [14] F. Remondino; S. El-Hakim. Image-based 3D modelling: a review. *Photogramm. Rec.* 21: 269–291 (2006).